ADVANCED ENERGY MATERIALS
www.advenergymat.de

Recyclable Fluorine-Free Water-Borne Binders for High-Energy Lithium-Ion Battery Cathodes

*Felix Leibetseder, Jingyu Xie, Elisabeth Leeb, Günter Hesser, Karl-Heinz Pettinger, and Klaus Bretterbauer**

The rapidly increasing demand for lithium-ion batteries and the fight against climate change call for novel materials that enhance performance, enable eco-friendly processing, and are designed for efficient recycling. In lithium-ion batteries, the binder polymer, used for cathode production, constitutes an integral but often overlooked component. The currently used polyvinylidene fluoride is processed with toxic organic solvents and has numerous other disadvantages concerning adhesion, conductivity, and recyclability. A change to aqueous processing using new, multi-functional, purpose-built materials that are soluble in water and fluorine-free would thus constitute an important advance in the battery sector. Herein, four water-soluble surfactant-like polymers based on 11-aminoundecanoic acid, that can be obtained in high purity and at a multigram scale are described. Free radical polymerization allows modification of the polymer with a wide variety of comonomers. The materials presented significantly enhance adhesion, are thermally stable at temperatures up to 350 °C, and are compatible with state-of-the-art high-energy $LiNi_{0.6}Mn_{0.2}Co_{0.2}O_2$ (NMC 622) cathode materials. It is also shown new recycling pathways made possible by the reversible pH-dependent water-solubility of the materials.

1. Introduction

A serious effort to fight the imminent climate crisis requires a reduction in CO_2 emissions on many emerging fronts, one of which is the electrification of the transportation sector.[1] Since in cars and trucks, high energy density and high capacity are of utmost importance, lithium-ion batteries (LIBs) have emerged as the best (commercially) available concept. However, huge challenges remain for optimizing batteries, especially in terms of capacity, long-term cycle stability, and safety.[1–4] Two other crucial improvements – green, sustainable production and efficient recycling – are of rapidly growing importance due to the drastic increase in global demand (projected to be > 30% p.a. until 2030).[2,5,6]

These challenges result in the need for new materials that can be implemented in the high-energy LIBs. Due to their intricate nature, LIBs entail numerous variables which need to be studied, changed, and tweaked including cathode[2,7,8] and anode materials,[2,9–12] electrolytes,[2] separators,[13] additives,[2,12,14] etc. A component that is often overlooked, but deserves attention is the electrode binder, or more precisely the cathode binder.[4] While anode binders received considerably more attention in recent years due to the increased material demands arising from promises of new anode materials such as silicon,[15–19] the lithium-ion battery cathode (LIBC) binder is underrepresented in the literature.[2]

Cathode binders must fulfill two obligatory requirements: First, they have to be electrochemically stable at voltages up to that of the cathode material. Second, they must provide adhesion between the cathode components and the aluminum current collector. Additionally, it has to be processable in a roll-to-roll process, which is affected by slurry viscosity, thermal stability, and solubility.[20,21]

The state-of-the-art material in LIBCs is polyvinylidene fluoride (PVDF), which is a fluorinated, electrochemically stable polymer. However, its adhesion to the current collector is poor,[22,23] and PVDF-based LIBCs are also currently processed in organic solvents, like *N*-methyl-2-pyrrolidone (NMP) – an expensive and toxic solvent with a high boiling point. This is suboptimal in terms of green processing and also leads to problems down the

F. Leibetseder, K. Bretterbauer
Institute for Chemical Technology of Organic Materials
Johannes Kepler University Linz
Altenbergerstraße 69, Linz 4040, Austria
E-mail: klaus.bretterbauer@jku.at
J. Xie, K.-H. Pettinger
Technology Centre for Energy Landshut University of Applied Sciences
Wiesenweg 1, 94099 Ruhstorf an der Rott, Germany
E. Leeb
Institute of Physical Chemistry and Linz Institute for Organic Solar Cells (LIOS)
Johannes Kepler University Linz
Altenbergerstraße 69, Linz 4040, Austria
G. Hesser
Center for Surface and Nanoanalytics
Johannes Kepler University Linz
Altenbergerstraße 69, Linz 4040, Austria
The ORCID identification number(s) for the author(s) of this article can be found under https://doi.org/10.1002/aenm.202401074

DOI: 10.1002/aenm.202401074

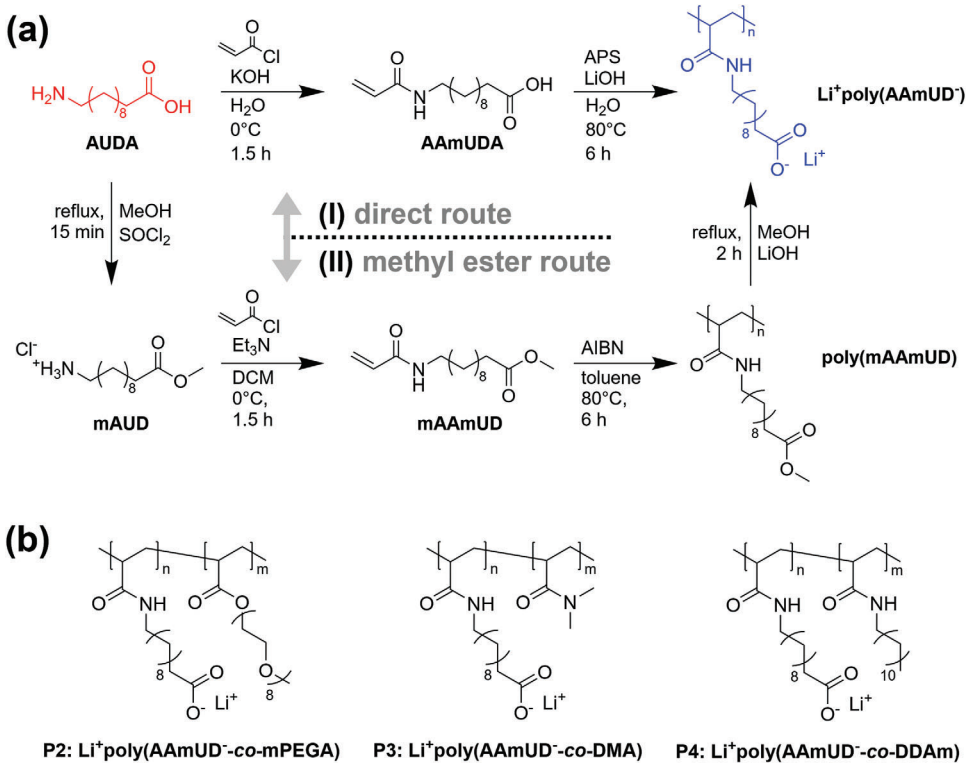

Figure 1. Reaction schemes for synthesizing the tailored binder polymers of interest and their corresponding structures. a) Reaction scheme of (I) direct synthesis of AAmUDA and subsequent polymerization to Li$^+$poly(AAmUD$^-$) (**P1**); (II) two-step methyl ester synthesis of mAUD, mAAmUD, and subsequent polymerization to **P1**; b) chemical structures of the binder polymers: Li$^+$poly(AAmUD$^-$-*co*-mPEGA) (**P2**), Li$^+$poly(AAmUD$^-$-*co*-DMA) (**P3**), Li$^+$poly(AAmUD$^-$-*co*-DDAm) (**P4**).

road for environmentally friendly recycling processes of spent materials.[3,6,21] These drawbacks, combined with the fact that it also provides no additional functionality to the LIB, make PVDF as a LIBC binder a prime candidate for an upgrade.

Current research in the field of LIBC binders mostly uses already widely available commercial polymers such as polyacrylic acid,[23,24] numerous biopolymers,[25–28] or their composites.[29,30] We describe a family of novel purpose-built multifunctional fluorine-free binders based on polymerizable surfactants. The presented materials are useable for 4.3 V versus Li/Li$^+$ LIBCs and can be processed in water. The polymers also demonstrate new options for their recycling.

2. Results and Discussion

The molecule of main interest in this work is 11-aminoundecanoic acid (AUDA). This compound, produced from the renewable feedstock castor oil, is an interesting bifunctional starting material and useful beyond the synthesis of polyamide 11. The reaction of AUDA with acryloyl chloride gives bench-stable solid monomers easily polymerizable through the free radical process. These polymers, neutralized with lithium hydroxide, bear lithium carboxylate groups attached to a polymer backbone over an aliphatic spacer – a combination of functional groups that promise properties such as good adhesion,[31] water solubility, electrochemical stability,[23,32] and the ability to scavenge protons.[23] In conjunction with the versatility of free radical (co)polymerization, these properties make the corresponding (co)polymers promising candidates for use as lithium-ion battery binders.

2.1. Synthesis of Monomers and Polymers

This section describes the direct reaction of AUDA with acryloyl chloride that yields 11-acrylamidoundecanoic acid (AAmUDA), and the synthesis of methyl 11-acrylamidoundecanoate (mAAmUD) (**Figure 1a**). The direct synthesis yielded 93% AAmUDA and mAAmUD was synthesized with an overall yield of 65% in two steps at purities greater than 99% (^{1}H-NMR). The synthesis of AAmUDA was adapted from previously reported procedures[33–35] the used solvents were changed, and the work-up procedure was optimized to allow an efficient scale-up to 40 g. The synthesis of mAAmUD directly from AUDA is described herein for the first time. The used solvents and work-up procedures were designed to accommodate a reaction scale of at least 25 g. Larger scales are also accessible, since the work-up procedures are straightforward (i.e., avoid column chromatography) and the reagents are affordable and readily available.

Direct addition of the acryloyl group was done in an aqueous solution. After acidification, the crude AAmUDA was conveniently removed via filtration, and the pure product was selectively dissolved with ethyl acetate. AAmUDA was then neutralized with LiOH and polymerized in aqueous solutions to

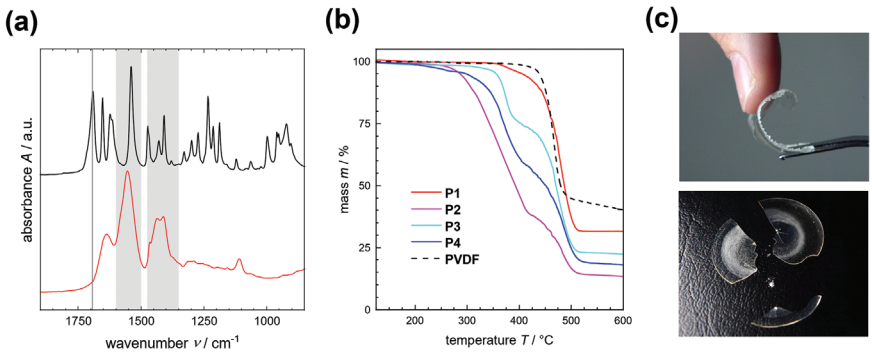

Figure 2. a) ATR-FTIR spectra of AAmUDA (black) and **P1** (red) indicating complete neutralization in the polymer by the absence of the carboxylic acid signal (ν, 1691 cm^{-1}) and presence of broad carboxylate signals ≈1550 (ν_s) and 1440 cm^{-1} (ν_{as}); changes are highlighted in light grey. b) TGA thermograms of the polymers **P1** (red), **P2** (magenta), **P3** (cyan), **P4** (blue), and reference material PVDF (dashed grey). The polymers **P2**-**P4** are thermally stable at temperatures up to 250 °C. **P1** even exhibits thermal stability comparable to PVDF. c) (top) Photograph of a dried solvent-cast sheet of the highly flexible copolymer **P2** bent by hand; (bottom) photograph of a solvent-cast plate of **P1** splintered by the impact of a screwdriver tip (video available in the Supporting Information). Copolymerization with mPEGA tailors the flexibility of the binder polymer, which is important to withstand volume change during charging and discharge of the battery.

obtain polymer binder Li^+poly($AAmUD^-$) (**P1**) The polymerization under aqueous conditions makes many polar comonomers accessible. In the methyl-ester route, the AUDA was first reacted under solventless conditions with methanol (MeOH), and thionyl chloride ($SOCl_2$) and methyl 11-amino undecanoate hydrochloride (mAUD) was obtained quantitatively. The excess of $SOCl_2$ and MeOH was simply removed *in vacuo*. The subsequent reaction with acryloyl chloride formed mAAmUD, which – unlike the unprotected monomer – is soluble in various organic solvents with polarities ranging from toluene to 1,4-dioxane. Usage of the protecting group scheme thus opens up the possibility of copolymerization with non-polar comonomers. The versatility of free radical polymerization in water and organic solvents allows purpose-built and tailored materials to be developed and is demonstrated below for tuning of various properties. We chose the three comonomers monomethyl ether poly(ethylene glycol) acrylate (mPEGA), *N,N*-dimethyl acrylamide (DMA), and *N*-dodecyl acrylamide (DDAm) reacted, respectively, at a 1:1 molar ratio with AAmUDA (or mAAmUD) to show the maximum impact of each comonomer on the resulting properties. Figure 1b illustrates the structures of the copolymer binders synthesized and studied: Li^+poly($AAmUD^-$-*co*-mPEGA) (**P2**), Li^+poly($AAmUD^-$-*co*-DMA) (**P3**), and Li^+poly($AAmUD^-$-*co*-DDAm) (**P4**). All comonomers chosen are either readily available or readily synthesized, they were also chosen to show the broad variety of possible comonomers. mPEGA was chosen because the polyethylene glycol motif is well known for its use in polymer electrolytes and is known to promote lithium-ion transport due to the coordination of lithium ions and the reported hopping mechanism.[36–38] DMA was used because it is known to be water soluble and has adhesive properties.[39,40] The possibility of using apolar comonomers was shown with DDAm. This was made possible by the aforementioned methyl deprotection route.

2.2. Chemical and Physical Characterization of the Binders

NMR and FTIR were employed for basic chemical characterization of the binder polymers. In the NMR spectrum, the absence of the acrylic double-bond signals between 6.20 and 5.55 ppm indicates high conversions (greater than 95%) of the polymerization reaction. The complete set of spectra is provided in the Figures S1–S7 (Supporting Information). In the final polymer, the IR-active C = O stretching vibration caused by the carboxylic acid at 1691 cm^{-1} is also no longer visible in the FTIR spectra. Instead, the broad signals ≈1550 and 1440 cm^{-1} appear, which are caused by the "one-and-a-half C = O" stretching (ν_{as} / ν_s) vibrations of the lithium carboxylate moiety formed.[41] A comparison of the ATR-FTIR spectra of AAmUDA and **P1** is shown in **Figure** 2a and the complete set of infrared spectra is provided in the Figure S8 (Supporting Information).

All polymers produced (**P1**-**P4**) were soluble in water up to ≈10 wt%. However, due to the surfactant-like structure of AAmUDA, the polymerization of AAmUDA in water gave polymers that give rise to turbid solutions. This is attributed to the formation of polymeric micelles during polymerization.[35] As expected, the turbidity occurred only for polymers obtained by aqueous polymerization and not for those obtained via the methyl-ester route polymerized in organic media. This very complex behavior has already been documented for similar materials in the literature,[35,42] but – as described below – we observed no negative effect of the turbid solution when using the polymers as LIBC binders. On the contrary, the surfactant-like nature of the materials presented may be advantageous for their use as LIBC binders. Due to their amphoteric properties, the binders promise uniform distribution throughout the electrodes and high compatibility with all electrode materials and the aqueous processing medium.

The thermal stability of the polymers was tested by thermogravimetric analysis (TGA) and was promising with decomposition temperatures above 350 °C for **P1**. Figure 2b shows that its stability was comparable to that of the reference material PVDF. The polymers **P2** and **P4** were still stable up to 250 °C. The lower thermal stability of polymer **P2** is mainly caused by the weaker ester bond (acrylate) in comparison to the amide (acrylamide) bonds of the other polymers. The two-step decomposition visible for all tested materials can be attributed to the cleavage of the side chains which happens at lower temperatures than the

decomposition of the polymer backbone. The thermal stabilities determined are well within the processing window of LIB electrodes and the operating range of LIB cells. Processability and safe use can therefore be assumed.

Further thermal characteristics were determined by differential scanning calorimetry (DSC). All polymers were measured in the range between −80 and 200 °C. For polymers **P1**, **P3**, and **P4**, no glass transition (T_g) or melting was detected in this range (Figure S9, Supporting Information). All three materials were obtained as brittle, white solids, which were ground to a fine powder before further processing and testing. The brittleness of polymers **P1**, **P3**, and **P4** hints at a T_g higher than the tested 200 °C. This observation is backed up by publications attributing such unusually high T_g values of similar materials to the electrostatic forces introduced by the ionic nature of the lithium carboxylate groups.[43] The incorporation of mPEGA, however, changed the mechanical properties and resulted in the flexible polymer **P2**. Again, no T_g was detected in the range measured (Figure S9, Supporting Information), but submerging a drop-cast film in liquid N_2 caused the very flexible material to splinter. This behavior hints at a T_g well below the DSC instrument limit of −80 °C. Thus, the mPEGA comonomer in **P2** provides good mechanical flexibility within the LIBC across its operating range. Also note the absence of endothermal melting signals, especially for **P2** and **P4**, which normally exhibit crystalline behavior.[44,45] Hence, all polymers tested are amorphous. This is especially advantageous in the case of **P2**, where the short PEG side chains (7-9 repeating units) may help with lithium-ion transport in the electrode and crystalline regions would hinder these transport mechanisms.

Drop-casting polymer **P1** resulted in a hard, brittle polymer sheet that shattered when bent or hit with a sharp object. **P2** in contrast formed very flexible sheets. Photographs of the mechanical behaviors of **P1** and **P2** are shown in Figure 2c, and a complementary video is available in the Supporting Information.

The literature states that higher molecular weights are generally preferable for electrode binders, and only shorter chains (< 24 kDa) lead to unsatisfactory results.[46,47] Determining the molecular weights of these AAmUDA polymers is difficult, and the different polarities of the (co)polymers produced make size-exclusion chromatography (SEC) for molecular weight determination unfeasible. According to the literature, however, similar polymers produced under comparable (aqueous) conditions result in molecular weights between 100 and 1000 kDa (M_w, $Đ \sim 2$).[35,48,49] These molecular weights are in an excellent range for electrode binders.[46,47] The exception is **P4,** which was produced via the methyl-ester pathway and was analyzable by SEC (in tetrahydrofuran using polystyrene standards) prior to the deprotection step. This gave a M_w of 68 kDa ($Đ = 6.7$) which is considerably smaller (with higher dispersity) than the value found in the literature for the polymer obtained via the aqueous direct route, but can still be considered sufficient for use as a binder.[46,47]

2.3. Electrochemical Characterization and Lithium-Ion Battery Application

One of the essential properties of a LIB binder polymer is adhesiveness. It must hold the electrode materials, which are active materials and conducting agents, together and keep them firmly attached to the current collector. If the binder fails, delamination or pulverization occurs, which directly leads to the failure of the battery cell.[50] The currently used PVDF cathode binder shows only weak adhesion to the aluminum current collector and must be implemented with various additives in order to prevent delamination.[23,51] All the potential binder polymers presented exhibit vastly enhanced adhesion and should thus be able to prevent adhesive failure of the cathode. All binders were processed into electrodes and **Figure 3a** shows the results of 90°-peel-off tests. The AAmUDA homopolymer **P1** exhibited an approximately six-fold increase in adhesive force. The introduction of 50 mol% DMA (**P3**), a known adhesion-enhancing monomer,[40] increased the adhesive strength of the electrodes to ten times that of the PVDF reference material. As expected, adhesion was weaker with **P2** and **P4** but still three and five times that of PVDF, respectively. Optical inspection of the electrodes after the peel-off tests predominantly found cohesive failure for the materials produced while PVDF peeled off almost completely from the electrodes (Figure 3b). These results demonstrate the effectiveness of these materials for use in LIB electrodes as a binder. The adhesive strength as well as the tailorable chemical composition makes the materials also interesting for future research in the field of silicon-based high-capacity anodes.[47,50,51]

Another aspect to consider in the design of new (cathode) binders is electrochemical stability – an area in which the predominantly used PVDF excels.[3,52–54] Since acrylamide-based binders are underreported for the LIB cathode, oxidative linear sweep voltammetry (OLSV) was used to determine the electrochemical stability of polymers **P1-P4** in the voltage operating window of modern LIBs. Pristine polymer films were drop-cast onto glassy carbon electrodes and measured in a three-electrode setup. The results between 3 and 4.5 V versus Li/Li^+ are plotted in Figure 3c. Most importantly, no oxidative signals were detected in comparison to the blank glassy carbon electrodes which were exposed only to the battery electrolyte. Polymers **P1**, **P2**, and **P3** even showed a lower current response in the > 4 V region. This can be explained by a passivating effect as described by Pieczonka et al.[23] Polymer **P2** exhibited a higher and a lower current response at 3 and 4.5 V, respectively. This can be explained by the PEG side chains, which increase the ionic conductivity and provide better chemical compatibility with the carbonate-based electrolyte solvents. The OLSV tests showed that the polymers are stable up to the 4.3 V versus Li/Li^+ voltage of state-of-the-art nickel-rich layered lithium nickel manganese cobalt oxides (NMC)-based cathode materials such as $LiNi_{0.6}Mn_{0.2}Co_{0.2}O_2$ (NMC622).[55]

The next step toward building a battery with new binders was electrode processing of the tested materials with NMC622 under aqueous conditions. This is however not as straightforward as with the currently used combination of PVDF and organic solvents. Two major challenges are the homogeneous and stable dispersion of all components in the electrode slurry and, especially for NMC-based cathodes, the alkaline pH of the aqueous slurry. The latter causes etching of the natural oxide layer of the aluminum current collector which leads to the production of hydrogen gas during formation and cycling. This problem and its effect on the battery is well documented in the literature, and although several solutions have been suggested no definitive approach has yet emerged.[56,57] Thus, to show the influence of the

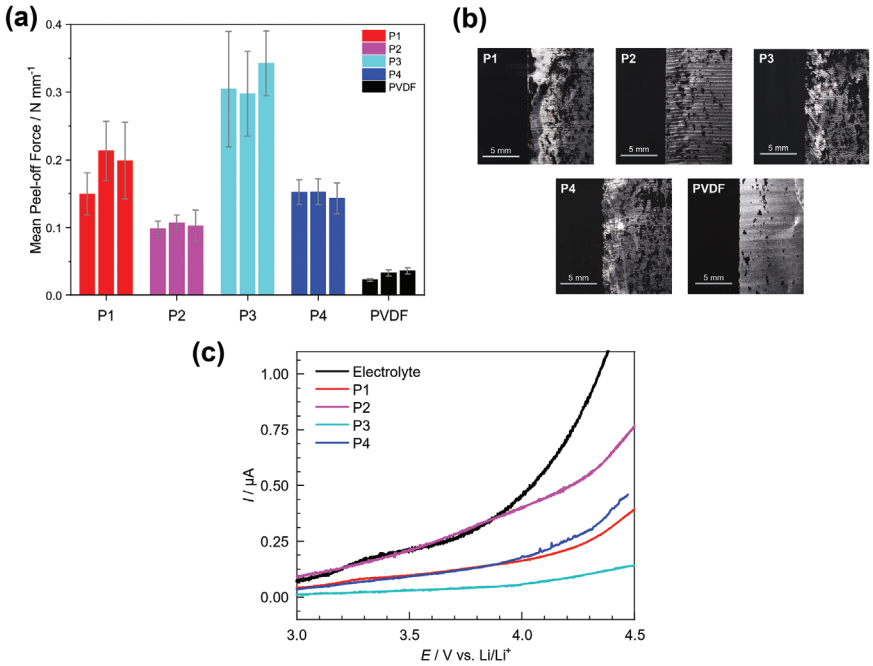

Figure 3. a) 90° peel-off adhesion tests of **P1** (red), **P2** (magenta), **P3** (cyan), **P4** (blue), and PVDF (black). Each bar represents the mean adhesion of a single measurement. The whiskers give the standard deviation of the single measurement.; b) photographs of electrodes after the peel-off tests **P1**-**P4** show cohesive breaks while PVDF shows adhesive failure; c) OLSV measurements of the pristine polymers drop-cast onto glassy carbon electrodes and measured against a Ag/AgCl quasi-reference and Pt as a counter electrode. Electrolyte (black), **P1** (red), **P2** (magenta), **P3** (cyan), and **P4** (blue).

binder on battery performance directly without the interference of secondary effects, it was decided not to add pH-regulating additives during processing.

Homogeneous dispersion of the active materials NMC and conductive carbon, however, was investigated closely because aiding this process is a defining feature of a binder. Scanning electron microscopy (SEM) images of the pristine cathodes, presented in **Figure** 4a, show a uniform distribution of NMC and conductive carbon (Figure 4a bottom right). The only remaining issue is the occurrence and inclusion of bubbles during the mixing and drying process (Figure 4a, top left, top right, bottom left), which was due to the slurry being mixed under atmospheric pressure. Although the prepared slurries were degassed while being static in a vacuum chamber, it was impossible to remove all the air inclusions at this late stage. The hydrophobic conductive carbon particles are agglomerating at the surface, creating isolated carbon-air structures (Figure S10, Supporting Information). This is sub-optimal in terms of the formation of a conducting network throughout the electrode. As reported in the literature, processing in water rather than NMP requires many adjustments, and both mixing and drying must be optimized extensively.[21] In the future, the removal of the air bubbles under reduced pressure

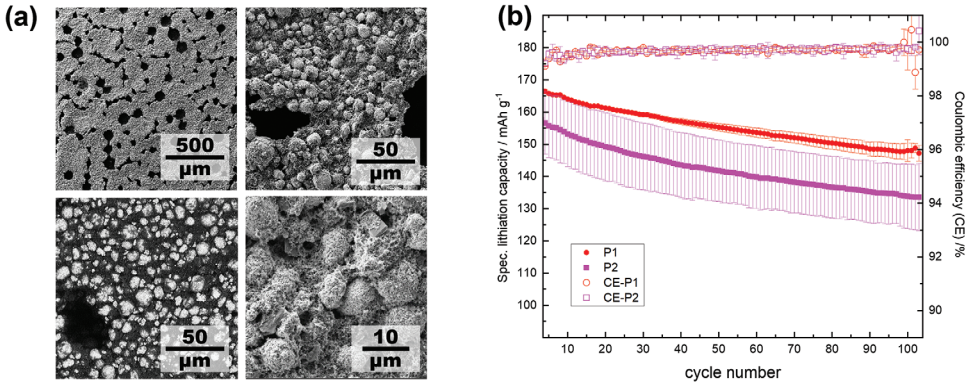

Figure 4. a) SEM images of pristine NMC622/**P1** electrodes recorded via secondary electron detector which shows the morphology (top left and right, bottom right), and via backscattering detector which shows the elemental contrast (bottom left) of the produced electrodes with binder **P1**; b) specific lithiation capacities (CCCV-mode) and coulombic efficiencies (CE) for half-cells (NMC622) with **P1** and **P2** as binder assembled in a coin cell configuration. The mean results of the four cells tested per binder are shown with whiskers indicating the standard deviation. 100 cycles were performed at a 0.1 C-rate.

toward the end of the mixing stage might be considered. Another promising chance is optimizing the electrode slurry mixing procedure by initially arranging the structures of conductive carbon and active material particles may assist in effectively forming a conducting network and eliminating air bubbles from the slurry. Despite the remaining challenges in terms of optimal coating, the produced electrodes were already sufficiently homogeneous and processable in order to be tested in battery cells.

The electrodes with polymers **P1** and **P2** were assembled in coin cell configurations using lithium metal as counter electrodes to demonstrate their electrochemical performance as LIBCs. The homopolymer **P1** was chosen for battery testing to establish the useability of AAmUDA-containing polymers, and **P2** was chosen due to increased ion conductivity and electrolyte compatibility of the PEG sidechains. Figure 4b shows the results of the battery tests in coin cells (specific lithiation capacities and coulombic efficiencies (CE)). The specific delithiation capacities of the cycling and cell-formation are shown in Figures S11 and S12 (Supporting Information). Charge and discharge curves for the 1st and 3rd formation cycle as well as the 100th cycle are shown in Figures S13 and S14 (Supporting Information). The results indicate a promising performance of the AAmUDA-based binders. The electrodes utilizing homopolymer **P1** retained 88.2% of their capacity after 100 cycles at a 0.1 C-rate. The ones containing the PEG copolymer **P2** showed a lower starting capacity (Δ10 mAh g^{-1}) but a similar capacity retention of ≈84.7%. As can be seen in Figure 4b the lower standard deviations seen for **P1** compared to **P2**, hint at a more uniform surface and an overall higher stability of battery cells using the electrodes with homopolymer **P1**. The coulombic efficiencies were close to 100% for all cycles recorded and cells measured after formation. Considering that the electrodes tested were not fully uniform and the high pH of the slurry was not adjusted, the results show excellent electrochemical performance and stability of the tested binders, especially of the homopolymer **P1**. If directly compared to published research in the field of aqueous cathode binders the presented materials are highly competitive with published capacity retentions of 80% – 90% with similar charge rates and cycles.[24–26]

Thus, the polymer binder **P1** is the first time polymers with surfactant-like sidechains are successfully utilized as LIBC binders. The binders are also useable up to 4.3 V versus Li/Li^+, which opens up many more use cases, for instance in the well-established and less demanding $LiFePO_4$ cathodes and even in sodium-ion batteries.[58] The application in high-voltage LMNO spinel cathodes[23] may also be considered. The tunable properties (adhesion, ionic-conductivity, or mechanical stability) of **P1** based on comonomer incorporation as shown for copolymers **P2**-**P4** offer potential for purpose-built, tailored materials.

2.4. Processing and Recycling Assessment

As the demand for LIBs is rapidly increasing, "green" processing and recycling are also important when designing new materials for devices. In this regard, the presented materials all exhibit several favorable properties. **P1** is used as the main example throughout this subchapter, but the copolymers **P2**-**P4** can be processed and recycled under the same conditions.

The currently used processing solvent NMP is high-boiling, expensive, toxic, and must be recovered fully to prevent release into the environment or harm to the operating personnel. Here, the advantage of water-soluble binders is evident, eliminating the need for solvent recovery. This leads to simpler and cheaper coater setups, increased safety for workers in the manufacturing plant, and lower energy consumption throughout the process.[3,21,59,60] It is shown that **P1** is processable and useable as a water-soluble, fluorine-free alternative to PVDF. Water solubility is also advantageous when recycling electrodes from spent LIBs. A possible strategy is schematically presented in **Figure 5**a. Electrodes processed with binder **P1** can be recycled efficiently by dissolving the polymer in neutral or weakly alkaline aqueous solutions (Figure 5b). The active materials are released from the current collector (Figure 5b) and can then be removed conveniently by centrifugation or filtration. This process recovers the aluminum current collector directly, and the active mass is obtained without fluoropolymers bound to it. The latter is a clear advantage in further hydro and pyrometallurgical treatment and subsequent recovery of valuable metals (Li, Co, Ni, and Mn).[61] Afterwards, the pH-dependent solubility of **P1** enables subsequent recovery of the polymer. By acidification of the remaining aqueous recycling solution, the binder is precipitated and recovered (Figure 5b). Video showing electrode dissolution and polymer reprecipitation is provided in the Supporting Information. **P1** and its copolymers are not only water-processable but also show significant improvements for binder recycling. The findings described above demonstrate that a holistic approach to binder design considers not only stability and performance but also "green" processing and recycling of spent materials.

3. Conclusion

Further improvement and development of LIBs will play a huge role in the fight against climate change and require materials that not only provide great performance but also enable green processing and efficient recycling. The currently used cathode binder PVDF is a prime example of a battery component that urgently requires a more sustainable alternative. We have presented four potential candidates that are novel polyelectrolyte LIBC binders based on 11-aminoundecanoic acid derived from sustainable sources. The materials developed are water-processable, fluorine-free, and useable for state-of-the-art 4.3 V NMC622 cathodes for high-energy batteries. The binder system investigated is also tailorable with a wide variety of comonomers via two synthesis pathways for polar and non-polar monomers. We have shown that comonomers can be used to tune properties such as mechanical behavior, thermal stability, adhesive strength, and ionic conductivity. The introduction of mPEGA (**P2**) is of particular interest, as it i) changes mechanical behavior, rendering an otherwise brittle polymer flexible, and ii) enhances ionic conductivity. DMA (**P3**) was found to be a good comonomer for increasing adhesive strength and even outperformed the already excellent **P1**.

Aqueous electrode processing will benefit from further improvement and adaptation to aqueous processing of parameters that are currently optimized for organic solvents. We have shown that **P1** and **P2** are suitable candidates as binders for NMC-based LIBCs, as they exhibit steady charge-discharge cycling up to 88.2% capacity retention after 100 cycles. In addition to

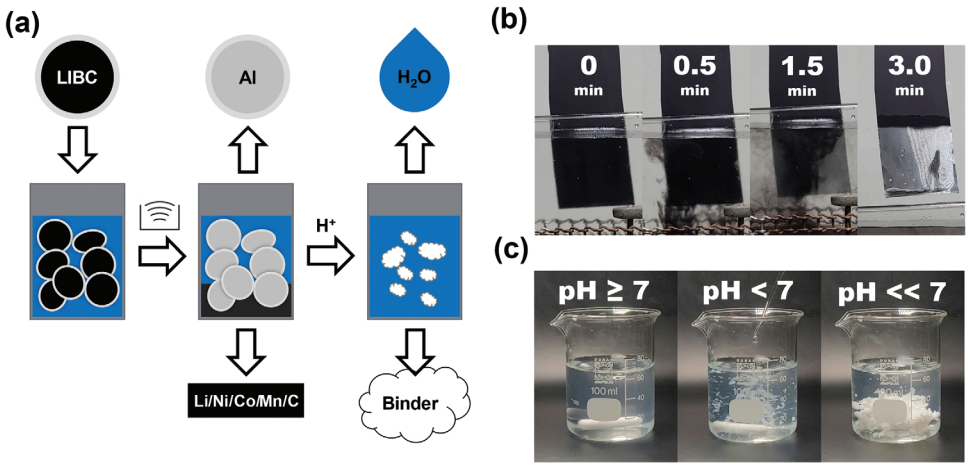

Figure 5. Recyclability of the new class of LIB binder materials presented. a) Scheme of a possible future recycling pathway enabled by our binders. LIBC can be submerged in water, and – after ultrasonication or mechanical treatment – aluminum foil can be recovered directly, while Li, Co, Ni, Mn, and conductive carbon can be recovered by filtration, and the remaining aqueous solution is treated with acid to recover the binder polymer. b) Electrodes dipped into water and ultrasonicated for 3 min. Photographs were taken before, during (at 0.5 and 1.5 min), and after the treatment (at 3 min). The pictures show the dissolving of the polymer, sedimentation of the active material, and recovery of the blank aluminum foil. c) Photographs showing the pH-dependent solubility for recovery of the polymer from aqueous solution. An aqueous polymer solution (1%) of **P1** is treated dropwise with an acid (10 % hydrochloric acid solution). **P1** precipitates in its protonated form and can be conveniently recovered by filtration.

tailorable binder properties (mechanical flexibility, adhesion, ion-conductivity), a main advantage of the AAmUDA-based polymers is their suitability for efficient recycling. Not only can the polymers be processed under aqueous conditions, but they also aid the recycling process because all materials developed show pH-dependent solubility. The binder in electrodes can therefore be dissolved under neutral/alkaline conditions, the clean aluminum current collector subsequently directly recovered, and the valuable metals lithium, cobalt, nickel, and manganese removed by filtration or centrifugation. The absence of polymer, and especially of fluoropolymer, aids the recycling of these materials immensely. The remaining binder in the solution can also be easily recovered by acidification of the solution, which causes immediate precipitation.

In summary, the materials presented open up a new pathway in binder design with green processing and recycling already in mind. Future tailoring of comonomer composition in combination with optimized electrode coating and drying promises purpose-built binders for greener, improved lithium-ion batteries.

4. Experimental Section

Synthesis of 11-Acrylamido Undecanoic Acid (AAmUDA): 11-Aminoundecanoic acid (AUDA, 40.0 g, 200 mmol) was suspended in an aqueous solution (500 mL) of sodium hydroxide (6.4 g, 0.53 mol). After 10 min of mixing with a mechanical stirrer at room temperature, the suspension was cooled in an ice bath, and acryloyl chloride (17.8 mL, ≈220 mmol) diluted with dichloromethane (20 ml) was added dropwise over the course of one hour. The reaction temperature was kept below 5 °C during acryloyl chloride addition and was subsequently warmed up to room temperature. After ≈1 h of total reaction time, the suspension was acidified with a 10% hydrochloric acid solution. The white precipitate was filtered, washed with distilled water, and dried in vacuo, affording pure (^{1}H-NMR) AAmUDA as a fine white powder (47.6 g, yield: 93 %).mp 79–81 °C, ^{1}H NMR (300 MHz, DMSO-d_6, 25 °C, δ/ppm): 11.96 (s, 1H, COOH), 8.04 (t, J = 5.4 Hz, NH), 6.21 (dd, $J1$ = 17.1,J_2 = 9.9 Hz,1H, CH = CH_2), 6.05 (dd, J_1 = 17.1, J_3 = 2.5 Hz, 1H, CH), 5.52 – 5.59 (dd, J_2 = 9.9, J_3 = 2.5 Hz, 1H, CH), 3.11 (m, 2H, CH_2), 2.19 (t, J = 7.3 Hz, 2H, CH_2), 1.15 – 1.55 (m, 16H); IR (Diamond-ATR): ν = 3350 – 2500 (m, ν(O-H)), 3301 (m, ν(N-H)), 3047 (w, ν(C-H)) 2921 (s, ν_{as}(C-H)), 2853 (s, ν_s(C-H)), 1691 (s, ν(C = O)), 1652 (s, ν(C = O)), 1621 (s), 1540 (s, δ(N-H), δ(C-H)), 1473 (m), 1429 (w), 1409 (m), 1329 (w), 1297 (w), 1272 (m), 1234 (s, ν(C-O)), 1213 (m), 1187 (m), 1120 (w), 1064 (w), 997 (m, ω(C-H)), 960 (m), 922 (m, δ(O–H)), 808 (w), 719 (w, ρ(C-H)), 680–650 cm^{-1} (m, δ(N-H)).

Synthesis of Methyl 11-Amino Undecanoate (mAUD): AUDA (20.00 g, 99.2 mmol) was suspended in methanol (100 mL). Under vigorous stirring thionyl chloride ($SOCl_2$, 11.0 mL, 152 mmol) was added dropwise. The resulting clear solution was subsequently refluxed for 15 min and the solvent together with unreacted $SOCl_2$ was removed under reduced pressure. The product, mAUD as its hydrochloride salt was obtained as a white powder (25.02 g, 100%) and was used without further purification. mp 153–155 °C, ^{1}H NMR (300 MHz, DMSO-d_6, 25 °C, δ/ppm): 7.85 (br, 3H, $^+NH_3$), 3.85 (s, 3H, CH_3), 2,75 (m, 2H, CH_2), 2.29 (t, J = 7.4 Hz 2H, CH_2) 1.2 –1.6 (m, 16H); IR (Diamond-ATR): ν = 3250 – 2700 (m, ν(N-H)), 2920 (s, ν_{as}(C-H)), 2850 (s, ν_s(C-H)), 1724 (s, ν(C = O)), 1610 (w, δ_{as}(N-H)), 1560 (m, δ(C-H)), 1510 (m, δ_s(N-H)), 1467 (m), 1444 (m), 1419 (w), 1375 (w), 1334 (m), 1305(m), 1276 (m), 1245 (s), 1211 (s), 1174 (s, ν(C-O)), 1097 (m), 1041 (w), 1001 (m), 971 (m), 939 (w), 885 (w), 725 (w, ρ(C-H)).

Synthesis of Methyl 11-Acrylamido Undecanoate (mAAmUD): mAUD hydrochloride (24.77 g, 98.4 mmol) was suspended in dichloromethane (130 ml) and triethylamine (30.0 ml, 219 mmol). The flask was flushed with argon, the solution was subsequently chilled in an ice bath, and acryloyl chloride (9.1 ml, 119 mmol) diluted with dichloromethane (20 mL) was added dropwise while maintaining temperatures below 10 °C. After the addition, the reaction mixture was warmed to room temperature and stirred for one additional hour. The white precipitate formed during the reaction was filtered off, and the organic phase was subsequently washed with 1 M HCl, distilled water, and 10 wt% $NaHCO_3$ solution. This was followed by a final wash step with brine. The organic layer was dried with sodium sulfate and the solvent was removed *in vacuo*. The crude product obtained was recrystallized with ethyl acetate. Additional product was recovered by washing the recrystallization residue with small amounts of diethyl ether. The solids obtained gave a yield of 17.33 g (65.4 % yield) of pure, white, crystalline mAAmUD product.

M.p.: 66–67 °C, ^{1}H NMR (300 MHz, DMSO-d_6, 25 °C, δ/ppm): 8.03 (t, J =,1H, NH), 6.20 (dd, J_1 = 17.1 Hz, J_2 = 10.0 Hz, 1H, CH), 6.05 (dd, J_1 = 17.1 Hz, J_3 = 2.5 Hz, 1H, CH), 5.55 (dd, J_2 = 10.0 Hz, J_3 = 2.5 Hz, 1H, CH), 3.58 (s, 1H, CH_3), 3.11 (m, 2H, CH_2), 2.29 (t, J = 7.4 Hz, 2H, CH_2), 1.60 – 1.15 (m, 16H); IR (Diamond-ATR): ν = 3261 (m, ν(N-H)), 3066 (w, ν(C-H)), 2952 (w), 2917 (s, ν_{as}(C-H)), 2896 (w), 2871 (w), 2846 (s, ν_s(C-H)), 1720 (s, ν(C = O)), 1668(m), 1652 (m, ν(C = O)), 1612 (m), 1550 (s, s, δ(N-H), δ(C-H)), 1473 (m), 1440 (m), 1411 (m), 1380 (m), 1334 (m), 1299 (w), 1272 (m), 1236 (s), 1207 (s), 1174 (s), 1114 (w), 985 (m), 962 (m), 919 (w), 885 (w), 810 (w), 704 (m).

Synthesis of N-Dodecylacrylamide (DDAm): DDAm was synthesized in full accordance with the previously reported procedure [45](69%). M.p.: 56.5 °C; ^{1}H NMR (300 MHz, $CDCl_3$, 25 °C, δ/ppm): 6.27 (dd, J1 = 17.0 Hz, J2 = 1.6 Hz, 1H, CH), 6.07 (dd, J1 = 17.0 Hz, J2 = 10.1 Hz, 1H, CH_2), 5.64–5.58 (m, 2H, CH_2 and NH), 3.32 (dt, J1 = 6.0 Hz, J2 = 7.1 Hz, 2H, CH_2), 1.55–1.48 (m, 2H, CH_2), 1.29–1.25 (m, 18H, CH_2), 0.87 (t, J = 6.9 Hz, 3H, CH_3).

*Synthesis of Lithium Poly(AAmUDA) (**P1**)*: Finely ground AAmUDA (11.05 g, 43.3 mmol) was suspended and neutralized in a solution of $LiOH.H_2O$ (1.82 g, 43.3 mmol) in water (250 mL). The mixture was stirred for one hour and then purged with nitrogen for 15 min. The milky reaction mixture was then heated to 80 °C, and ammonium persulfate (APS, 120 mg, 1 wt%) was added. The solution turned clear over the course of 30 min. After 6 h of total reaction time, the solution was cooled, and the polymer was precipitated in a 10-fold excess of acetonitrile. The polymer was dried in a vacuum drying cabinet at 40 °C and was obtained as a white solid (11.38 g, 100 % yield).

*Synthesis of Lithium Poly(AAmUDA-co-mPEGA) (**P2**)*: Analog for the procedure for **P1** a copolymer of 50 mol% AAmUDA and mPEGA was prepared. The mPEGA was added before the polymerization solution was heated up. The polymer was recovered after the solvent was removed in a vacuum and the polymer was further dried at 40 °C in a vacuum cabinet.

*Synthesis of Lithium Poly(AAmUDA-co-DMA) (**P3**)*: The polymer **P3** was prepared analog to the procedure described for **P2**. Instead of mPEGA, 50 % *N*,*N*-dimethylacrylamide (DMA) is used.

*Synthesis of Lithium Poly(AAmUDA-co-DDAm) (**P4**)*: For the preparation of the polymer **P4,** mAAmUD and DDAm were dissolved in benzene. The solution was purged with nitrogen for 15 min and subsequently heated up. At reflux 1 wt% AIBN was added to the solution and the reaction proceeds for 6 h under argon. Afterwards, the solvent was removed under vacuum and the polymer was redissolved in MeOH. Two equivalents of potassium hydroxide (KOH) were added to the solution and the mixture was refluxed for 2 h. The resulting solution was precipitated into an excess of 1 M aqueous HCl solution. The precipitate was then washed and suspended in deionized water. Lithium hydroxide was added until the polymer was fully dissolved, and the solution remained slightly alkaline. The removal of the solvent gives **P4**.

Electrode Preparation: The water-based slurries were prepared using a dissolver (Dispermat, VMA-Getzmann, Germany). The solid content of all slurries produced was kept at 63.5 wt%. The solid components contained 5 wt% fluorine-free polymer binder (**P1** / **P2**), 90 wt% NCM 622 active material (NCM 622 DT011, BASF, Germany), 4 wt% conductive black Super C65 (Imerys, France) and 1 wt% conductive graphite (KS6L, TIMCAL, Switzerland). The final slurry was then coated onto an aluminum foil (20 µm, Gelon LIB, China) using a laboratory knife coater. The continuously roll-to-roll coated electrodes were dried in a 2 m drying tunnel with 4 temperature-controlled zones (40 °C/60 °C/80 °C/100 °C). The loading of electrode **P1** was 1.76 ± 0.02 mAh cm^{-2} and of the electrode **P2** it was 1.7 ± 0.02 mAh cm^{-2} (based on 176 mAh g^{-1} for NMC622). The mass loadings of the electrodes are 10.1 ±0.1 mg cm^{-2} for **P1** and 9.6 ±0.1 mg cm^{-2} for **P2**.

Coin Cell Assembly: Electrode samples were prepared using a handheld punch (Nogamigiken, Japan) with a diameter of 12 mm. Following the initial drying process at 110 °C under vacuum for 12 h, and weighing immediately afterwards, the samples underwent a second drying cycle at 45 °C under vacuum overnight. Subsequently, the electrodes were assembled as working electrodes into 2032-type coin cells within an argon Glovebox (MB20G, MBraun, Germany), with lithium metal disks (14 mm) as counter electrodes (GELON LIB CO., LIMITED, China). Two separators (VWR glass fiber 691, USA) with a size of 16 mm were positioned between the electrodes, soaked with 80 µL of electrolyte. The electrolyte LP57 (Gotion Inc., China) is a solution of 1 M $LiPF_6$ in ethylene carbonate and ethyl methyl carbonate (EC:EMC) in a weight ratio of 30:70 wt%. The electric crimping machine (DF160, Cambridge Energy Solutions LTD., United Kingdom) applied 800 kg force to seal the cell.

Electrochemical Tests: The electrochemical tests were conducted with a battery cycler (BaSyTec, Germany) in coin cells at 25 °C. The cycling potential was between 3 and 4.3 V versus Li/Li$^+$. For half-cell charging (lithiation), galvanostatic (CC) and potentiostatic (CV) modes were used. CV charging steps were continued until the charging current dropped below 0.05 C-rate. For the discharging (delithiation) process, only the CC mode was used. The formation started after 12 h wetting time and ended after three cycles. Subsequently, the cycling tests ran for another 100 cycles. For both formation and cycling tests, the electrodes were cycled at 0.1 C-rate (symmetrically). 1 C was based on the theoretical capacity of the active material NCM622, which was 176 mAh g^{-1} and the weight content of the active material in the electrode, which was 90%.

Further Material Characterization: All reagents and solvents were purchased from standard chemical suppliers in reagent quality and were used without further purification. All NMR spectra were recorded in DMSOd6, $CDCl_3$, CD_3OD, or D_2O on a 300 MHz Bruker Avance spectrometer using standard pulse programs as provided by the manufacturer. Signals were referenced to the corresponding solvent signals. A Mettler Toledo DSC 3+ equipped with a TC 100 IntraCooler was used for thermal analysis of the polymers. Heat-cool-heat cycles between −80 and 150 °C (up to 200 °C for AAmUDA) were performed. The heating/cooling rate was 10 °C min^{-1}. Fourier-transform infrared spectroscopy (FTIR) was performed on a Thermo Electron Nicolet 5700 spectrometer with a Specac Golden Gate High-Temperature Attenuated Total Reflectance (ATR) sampling unit. The electrochemical stability of the pristine polymers was determined by oxidative linear sweep voltammetry (OLSV). The polymers were drop-casted onto glassy carbon electrodes and measured in 1 M $LiPF_6$ EC/DMC 1:1 solution against a quasi-reference Ag/AgCl electrode. A platinum counter electrode was employed. After each OLSV measurement, the system was calibrated with ferrocene. Peel-off tests were conducted with pristine electrodes. The electrodes were taped with 3 M 467 MP double-side adhesive tape onto a moveable plate with a 1.2 kg metal roller. The adhesive force was measured at a 90° angle with a Zwick-Roell tensile tester. The recycling tests (dissolution and reprecipitation) were also conducted with pristine electrodes.

Supporting Information

Supporting Information is available from the Wiley Online Library or from the author.

Acknowledgements

The authors thank Prof. Niyazi Serdar Sariciftci (Institute of Physical Chemistry and Linz Institute for Organic Solar Cells) for his support and help with electrochemical stability measurements. The authors also would also like to thank Doris Danninger and Prof. Martin Kaltenbrunner (Soft Matter Physics Division, Institute of Experimental Physics) for assisting with the adhesion measurements. The used NMR spectrometers were acquired in collaboration with the University of South Bohemia (CZ) with financial support from the European Union through the EFRE INTERREG IV ETC-AT-CZ program (project M00146, "RERI-uasb").

Conflict of Interest

The authors declare no conflict of interest.

Data Availability Statement

The data that support the findings of this study are available from the corresponding author upon reasonable request.

Keywords

aqueous processing, fluorine-free, lithium-Ion battery, multifunctional binders, polyelectrolytes

Received: March 8, 2024
Revised: April 18, 2024
Published online:

[1] J. B. Goodenough, K.-S. Park, *J. Am. Chem. Soc.* **2013**, *135*, 1167.
[2] M. Armand, P. Axmann, D. Bresser, M. Copley, K. Edström, C. Ekberg, D. Guyomard, B. Lestriez, P. Novák, M. Petranikova, W. Porcher, S. Trabesinger, M. Wohlfahrt-Mehrens, H. Zhang, *J. Power Sources* **2020**, *479*, 228708.
[3] N. Lingappan, L. Kong, M. Pecht, *Renewable Sustainable Energy Rev.* **2021**, *147*, 111227.
[4] S.-L. Chou, Y. Pan, J.-Z. Wang, H.-K. Liu, S.-X. Dou, *Phys. Chem. Chem. Phys.* **2014**, *16*, 20347.
[5] J. Fleischmann, M. Hanicke, E. Horetsky, D. Ibrahim, S. Jautelat, M. Linder, P. Schaufuss, L. Torscht, A. Rijt, *McKinsey & Company* **2023**.
[6] W. Dou, M. Zheng, W. Zhang, T. Liu, F. Wang, G. Wan, Y. Liu, X. Tao, *Adv. Funct. Mater.* **2023**, *33*, 2305161.
[7] W. He, W. Guo, H. Wu, L. Lin, Q. Liu, X. Han, Q. Xie, P. Liu, H. Zheng, L. Wang, X. Yu, D.-L. Peng, *Adv. Mater.* **2021**, *33*, 2005937.
[8] J. U. Choi, N. Voronina, Y.-K. Sun, S.-T. Myung, *Adv. Energy Mater.* **2020**, *10*, 2002027.
[9] H. Cheng, J. G. Shapter, Y. Li, G. Gao, *J. Energy Chem.* **2021**, *57*, 451.
[10] C. Zhang, F. Wang, J. Han, S. Bai, J. Tan, J. Liu, F. Li, *Small Struct* **2021**, *2*, 2100009.
[11] L. Sun, Y. Liu, R. Shao, J. Wu, R. Jiang, Z. Jin, *Energy Storage Mater.* **2022**, *46*, 482.
[12] G. G. Eshetu, E. Figgemeier, *ChemSusChem* **2019**, *12*, 2515.
[13] C. M. Costa, Y.-H. Lee, J.-H. Kim, S.-Y. Lee, S. Lanceros-Méndez, *Energy Storage Mater.* **2019**, *22*, 346.
[14] H. Zhao, X. Yu, J. Li, B. Li, H. Shao, L. Li, Y. Deng, *J. Mater. Chem. A* **2019**, *7*, 8700.
[15] S. Li, Y.-M. Liu, Y.-C. Zhang, Y. Song, G.-K. Wang, Y.-X. Liu, Z.-G. Wu, B.-H. Zhong, Y.-J. Zhong, X.-D. Guo, *J. Power Sources* **2021**, *485*, 229331.
[16] A. N. Preman, H. Lee, J. Yoo, I. T. Kim, T. Saito, S. Ahn, *J. Mater. Chem. A* **2020**, *8*, 25548.
[17] Y. Yang, S. Wu, Y. Zhang, C. Liu, X. Wei, D. Luo, Z. Lin, *Chem. Eng. J.* **2021**, *406*, 126807.
[18] Y.-M. Zhao, F.-S. Yue, S.-C. Li, Y. Zhang, Z.-R. Tian, Q. Xu, S. Xin, Y.-G. Guo, *InfoMat* **2021**, *3*, 460.
[19] L. Deng, Y. Zheng, X. Zheng, T. Or, Q. Ma, L. Qian, Y. Deng, A. Yu, J. Li, Z. Chen, *Adv. Energy Mater.* **2022**, *12*, 2200850.
[20] F. Zou, A. Manthiram, *Adv. Energy Mater.* **2020**, *10*, 2002508.
[21] D. L. Wood, J. D. Quass, J. Li, S. Ahmed, D. Ventola, C. Daniel, *Dry. Technol.* **2018**, *36*, 234.
[22] D. Jeong, D.-S. Kwon, H. J. Kim, J. Shim, *Adv. Energy Mater.* **2023**, *13*, 2302845.
[23] N. P. W. Pieczonka, V. Borgel, B. Ziv, N. Leifer, V. Dargel, D. Aurbach, J.-H. Kim, Z. Liu, X. Huang, S. A. Krachkovskiy, G. R. Goward, I. Halalay, B. R. Powell, A. Manthiram, *Adv. Energy Mater.* **2015**, *5*, 1501008.
[24] J.-H. Kuo, C.-C. Li, *J. Electrochem. Soc.* **2020**, *167*, 100504.
[25] Q. Gan, N. Qin, H. Guo, F. Zhang, H. Yuan, W. Luo, Z. Li, Y. Li, L. Lu, Z. Xu, L. Wang, J. Lu, Z. Lu, *ACS Energy Lett.* **2024**, *9*, 1562.
[26] A. C. Rolandi, C. Pozo-Gonzalo, I. de Meatza, N. Casado, M. Forsyth, D. Mecerreyes, *ACS Appl. Energy Mater.* **2023**, *6*, 8616.
[27] N. Loeffler, J. von Zamory, N. Laszczynski, I. Doberdo, G.-T. Kim, S. Passerini, *J. Power Sources* **2014**, *248*, 915.
[28] G. Zhang, B. Qiu, Y. Xia, X. Wang, Q. Gu, Y. Jiang, Z. He, Z. Liu, *J. Power Sources* **2019**, *420*, 29.
[29] L. Rao, X. Jiao, C.-Y. Yu, A. Schmidt, C. O'Meara, J. Seidt, J. R. Sayre, Y. M. Khalifa, J.-H. Kim, *ACS Appl. Mater. Interfaces* **2022**, *14*, 861.
[30] J. Mo, D. Zhang, M. Sun, L. Liu, W. Hu, B. Jiang, L. Chu, M. Li, *Polymers (Basel)* **2021**, *13*, 3992.
[31] D. W. Aubrey, S. Ginosatis, *J. Adhes.* **1981**, *12*, 189.
[32] J.-H. Lee, U. Paik, V. A. Hackley, Y.-M. Choi, *J. Power Sources* **2006**, *161*, 612.
[33] I. M. Zorin, T. S. Reznichenko, A. Y. Bilibin, *Polym. Bull.* **2006**, *57*, 57.
[34] K. W. Yeoh, C. H. Chew, L. M. Can, L. L. Koh, H. H. Teo, *J. Macromol. Sci., Chem.* **1989**, *26*, 663.
[35] N. V. Tsvetkov, L. N. Andreeva, I. M. Zorin, S. V. Bushin, E. V. Lebedeva, I. A. Strelina, M. A. Bezrukova, A. A. Lezov, I. A. Makarov, A. Y. Bilibin, *Polym. Sci. Ser. A* **2011**, *53*, 355.
[36] D. Diddens, A. Heuer, O. Borodin, *Macromolecules* **2010**, *43*, 2028.
[37] J. Chattoraj, M. Knappe, A. Heuer, *J. Phys. Chem. B* **2015**, *119*, 6786.
[38] O. Borodin, G. D. Smith, *Macromolecules* **2006**, *39*, 1620.
[39] L. Wang, S. Liu, J. Cheng, Y. Peng, F. Meng, Z. Wu, H. Chen, *Soft Matter* **2022**, *18*, 6115.
[40] C. Fang, Y. Jing, Y. Zong, Z. Lin, *Int. J. Adhes. Adhes.* **2016**, *71*, 105.
[41] B. C. Smith, *Spectroscopy* **2018**, *33*, 20.
[42] N. V. Tsvetkov, L. N. Andreeva, E. V. Lebedeva, I. A. Strelina, A. A. Lezov, A. N. Podseval'nikova, N. G. Mikusheva, V. O. Ivanova, I. A. Makarov, I. M. Zorin, A. Y. Bilibin, *Polym. Sci. Ser. A* **2011**, *53*, 666.
[43] T. Tsutsui, T. Tanaka, *Polymer* **1977**, *18*, 817.
[44] S. Sundararajan, A. B. Samui, P. S. Kulkarni, *React. Funct. Polym.* **2018**, *130*, 43.
[45] F. Leibetseder, J. Bičvić, K. Bretterbauer, *Monatsh. Chem.* **2023**, *154*, 497.
[46] B. Hu, I. A. Shkrob, S. Zhang, L. Zhang, J. Zhang, Y. Li, C. Liao, Z. Zhang, W. Lu, L. Zhang, *J. Power Sources* **2018**, *378*, 671.
[47] D. Yao, J. Feng, J. Wang, Y. Deng, C. Wang, *J. Power Sources* **2020**, *463*, 228188.
[48] Y. Han, J. Tan, D. Wang, K. Xu, H. An, *J. Appl. Polym. Sci.* **2019**, *136*, 47581.
[49] K. W. Yeoh, C. H. Chew, L. M. Can, L. L. Koh, H. H. Teo, *J. Macromol. Sci., Chem.* **1989**, *26*, 663.
[50] N. Lingappan, L. Kong, M. Pecht, *Renewable Sustainable Energy Rev.* **2021**, *147*, 111227.
[51] J. Hu, Y. Wang, D. Li, Y.-T. Cheng, *J. Power Sources* **2018**, *397*, 223.
[52] L. Chen, S. Venkatram, C. Kim, R. Batra, A. Chandrasekaran, R. Ramprasad, *Chem. Mater.* **2019**, *31*, 4598.
[53] Q. Zhou, J. Ma, S. Dong, X. Li, G. Cui, *Adv. Mater.* **2019**, *31*, 1902029.
[54] A. Kraytsberg, Y. Ein-Eli, *Adv. Energy Mater.* **2012**, *2*, 922.
[55] R. Jung, M. Metzger, F. Maglia, C. Stinner, H. A. Gasteiger, *J. Phys. Chem. Lett.* **2017**, *8*, 4820.
[56] M. Bichon, D. Sotta, N. Dupré, E. de Vito, A. Boulineau, W. Porcher, B. Lestriez, *ACS Appl. Mater. Interfaces* **2019**, *11*, 18331.
[57] A. Kazzazi, D. Bresser, A. Birrozzi, J. von Zamory, M. Hekmatfar, S. Passerini, *ACS Appl. Mater. Interfaces* **2018**, *10*, 17214.
[58] Q. Wang, J. Li, H. Jin, S. Xin, H. Gao, *InfoMat* **2022**, *4*, e12311.
[59] A. Cholewinski, P. Si, M. Uceda, M. Pope, B. Zhao, *Polymers* **2021**, *13*, 631.
[60] A. Guerfi, M. Kaneko, M. Petitclerc, M. Mori, K. Zaghib, *J. Power Sources* **2007**, *163*, 1047.
[61] M. Wang, K. Liu, J. Yu, Q. Zhang, Y. Zhang, M. Valix, D. C. W. Tsang, *Glob. Chall.* **2023**, *7*, 2200237.